Generation of thrust and lift with airfoils in plunging and pitching motion

M.Moriche, O.Flores, M.García-Villalba

Departamento de Bioingeniería e Ingeniería Aeroespacial, Universidad Carlos III de Madrid

E-mail: mmoriche@ing.uc3m.es

Abstract.

We present fully resolved Direct Numerical Simulations of 2D flow over a moving airfoil, using an in-house code that solves the Navier-Stokes equations of the incompressible flow with an Immersed Boundary Method. A combination of sinusoidal plunging and pitching motions is imposed to the airfoil. Starting from a thrust producing case (Reynolds number, $Re = 1000$, reduced frequency, $k = 1.41$, plunging amplitude $h_0/c = 1$, pitching amplitude $\theta_0 = 30^\circ$, phase shift $\phi = 90^\circ$), we increase the mean pitching angle (in order to produce lift) and vary the phase shift between pitching and plunging (to optimize the direction and magnitude of the net force on the airfoil). These cases are discussed in terms of their lift coefficient, thrust coefficient and propulsive efficiency.

1. Introduction

Flight performance of small birds and insects is very attractive for aerodynamicists, specially in terms of maneuverability. These small animals produce thrust, lift and position control by flapping their wings and adjusting their body position. Similar strategies are being used in bio-inspired Micro Aerial Vehicles (MAVs), which are small unmanned aircrafts with sizes of the order of 15 cm. These flight devices have received a lot of attention in the last years, since equipped with a camera and some sensors they can be used for surveillance and reconnaissance missions in hazardous environments like bush fires or nuclear accidents. Due to their small size, the Reynolds number (Re) that characterizes MAVs flight is typically $10^2 - 10^4$, similar to that of small birds and insects [1]. Improving our understanding of flapping wings at low Re is a key factor to unlock the standardized design of bio-inspired MAVs, with the potential to achieve high maneuverability and efficiency in their flapping flight.

It is important to realise that this low Re combined with high amplitude flapping motions lead to an unsteady flight regime where massive flow separation is present. Under these conditions, unsteady aerodynamic mechanisms such as leading edge vortex, clap and fling and wake recapture are dominant [2]. The classical unsteady aerodynamic models for fixed wings are no longer valid, since they are designed for high Re, low amplitude motions.

Our capability to predict the aerodynamic forces for a flapping wing at low Re is very limited, and only Direct Numerical Simulations (DNS) are able to deliver reliable predictions. There are essentially no appropriate low order models, mainly because of the vast parameter space of flapping flight. Although there have been a large number of studies (see the reviews of [3] and [4]) the mapping of that parametric space is sparse.

In the present paper, we consider the pitching and plunging motion of 2D airfoils. In particular, we focus on the balance between the lift and thrust, and in how a thrust generation case can be converted into lift generation by changing the mean pitching angle.

2. Numerical method

The simulations presented here have been developed using an in-house code that solves the Navier Stokes equations for an incompressible flow, using a fractional step method in a staggered grid. The presence of solid boundaries (airfoil) is modelled using the direct-forcing Immersed Boundary Method proposed by Uhlmann [5]. The code is written in Fortran and uses MPI (for parallelization) and HYPRE libraries (for the solution of the linear systems). The code has been extensively validated, as reported by Moriche [6].

In the following, we present two-dimensional (2D) simulations of a NACA-0012 airfoil of chord c immersed in a free stream of velocity U_∞, flapping with a sinusoidal plunging and pitching motion. The computational domain has a size of $25c$ in the streamwise direction and $15c$ in the vertical direction. The number of grid points is 3200 in the streamwise direction and 1920 in the vertical direction. This number has been selected based on preliminary simulations to properly predict the aerodynamic forces. We employ a Dirichlet boundary condition at the inflow plane, free slip at the top and bottom boundaries and a convective boundary condition at the outflow plane.

The plunging motion is imposed by the vertical displacement of the quarter chord point of the airfoil

$$h(t) = h_0 \sin\left(2\pi f\, t\right), \tag{1}$$

where h_0 is the plunging amplitude and f is the oscillation frequency. The pitching motion is imposed by the angle of the chord line of the airfoil with the streamwise direction

$$\theta(t) = \theta_m + \theta_0 \sin\left(2\pi f\, t + \phi\right), \tag{2}$$

where θ_m is the mean pitching value, θ_0 the pitching amplitude and ϕ the pitching phase shift. Using c and U_∞ as characteristic dimensions, the airfoil kinematics is characterized by the following non-dimensional parameters: the Reynolds number $Re = U_\infty\, c/\nu$, the reduced frequency $k = 2\pi f\, c/U_\infty$, the plunging amplitude h_0/c, the pitching amplitude θ_0, the mean pitching value θ_m and the phase shift ϕ.

3. Results

We have performed a series of simulations in which Re, k, h_0/c and θ_0 are kept constant, while we vary θ_m and ϕ. The aim is to evaluate how these two parameters influence the lift production, tilting and modulating the net force produced by the airfoil. We start from a thrust producing case that is taken as reference, case C0, and which corresponds to one of the cases reported by Anderson [7], except for a somewhat lower Reynolds number: $Re = 1000$, $\theta_0 = 30°$, $h_0/c = 1$ and $k = 1.41$. We then vary θ_m in the range (0° - 20°) and ϕ in the range (30° - 110°), to produce a database with 15 different cases.

A summary of the results obtained is presented in figure 1 which shows the values of the averaged lift (c_l) and thrust (c_t) coefficients. The solid (dashed) lines join points that correspond to cases with the same θ_m (ϕ). Finally, the color indicates the propulsive efficiency defined as

$$\eta = \frac{U_\infty \int_0^T c_t(t)\, dt}{\int_0^T c_l(t)\, \dot{h}(t)\, dt}, \tag{3}$$

where $c_l(t)$ and $c_t(t)$ are the instantaneous lift and thrust coefficients, $\dot{h}(t)$ is the vertical velocity of the quarter chord point and $T = 1/f$.

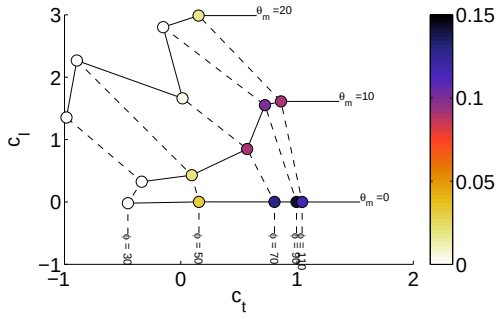

Figure 1. Averaged c_l versus averaged c_t. The color corresponds to the propulsive efficiency.

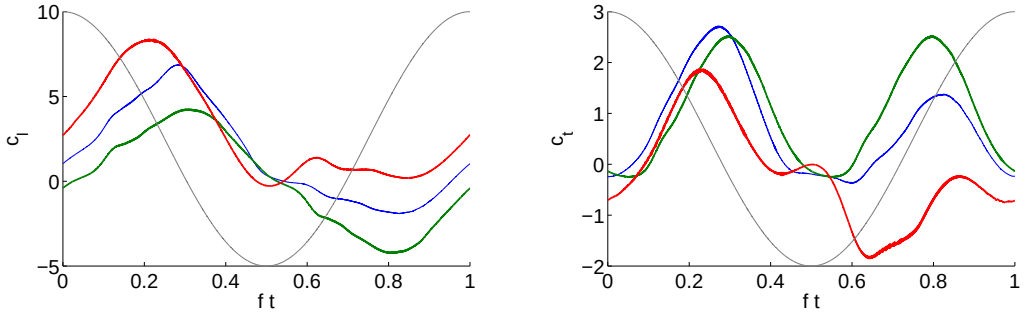

(a) (b)

Figure 2. Time history of force coefficients for selected cases with $\phi = 90°$. (a) c_l, (b) c_t. ——— $\theta_m = 10°$ (C1). ——— $\theta_m = 0°$ (C0). ——— $\theta_m = 20°$. The grey line corresponds to the vertical position of the quarter chord point in arbitrary units.

We can observe in figure 1 that for $\theta_m = 0°$, thrust is only produced for $\phi \gtrsim 50°$. Increasing ϕ up to the maximum value considered $\phi = 110°$, c_t increases but the propulsive efficiency reaches a maximum at $\phi = 90°$, note that this is the reference case (C0). Increasing θ_m leads, in general, to lift production at the expense of losing thrust. We select as optimal lift-production case (C1) the case with $\theta_m = 10°$, $\phi = 90°$, since the propulsive efficiency is comparable to C0, and c_l and c_t are of order unity.

In order to analyze the influence of θ_m and ϕ, figures 2 and 3 display the time history of the instantaneous force coefficients for selected cases. Figure 2 shows cases with $\phi = 90°$ and $\theta_m = 0°, 10°$ and $20°$. Recall that C0 ($\theta_m = 0°$) is the reference thrust producing case, and accordingly thrust is produced symmetrically both in the downstroke and the upstroke (see grey line for plunge position reference). In C1 ($\theta_m = 10°$), a similar amount of thrust is produced in the downstroke (compared to C0) and a somewhat lower amount of thrust is produced in the upstroke. Note that the lift is mainly produced in the downstroke, as expected. Further increasing θ_m to 20° we observe that much more lift is produced in the downstroke, while roughly no vertical force is produced in the upstroke. In terms of thrust, c_t is lower in the downstroke compared to C0 and C1. However, the main difference between $\theta_m = 20°$ and C0/C1 is that in the upstroke the former has a negative thrust (drag), resulting in a much lower averaged c_t.

Figure 3 shows cases with $\theta_m = 10°$ and $\phi = 70°, 90°$ and $110°$. It can be observed that overall, the effect of ϕ is less pronounced than the effect of θ_m. The cases with $\phi = 90°$ (C1) and $\phi = 110°$ are rather similar, since the latter produces more lift in the downstroke, which is lost

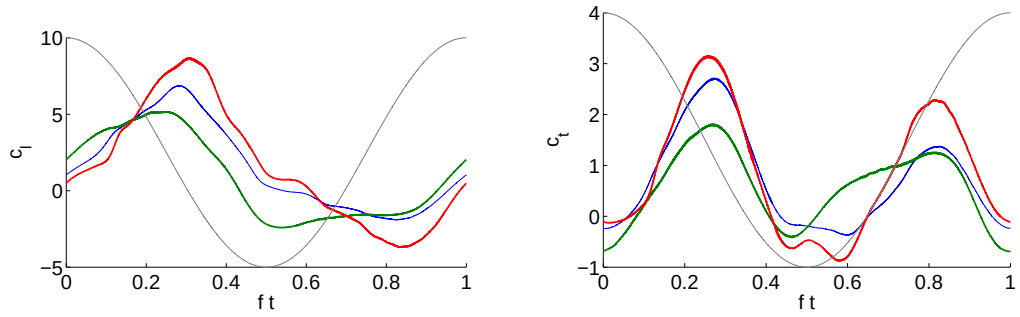

Figure 3. Time history of force coefficients for selected cases with $\theta_m = 10°$. (a) c_l, (b) c_t. ——— $\phi = 90°$ (C1). ——— $\phi = 70°$. ——— $\phi = 110°$. The grey line corresponds to the vertical position of the quarter chord point in arbitrary units.

in the upstroke. This results in a slightly lower propulsive efficiency that for C1. Concerning the thrust, the case with $\phi = 110°$ produces more thrust in both downstroke and upstroke, but this advantage is partially cancelled out by a worse performance in the downstroke to upstroke transition. Finally, the case with $\phi = 70°$ produces less lift and thrust than the other two cases, specially in the downstroke.

4. Conclusions

We have performed a series of DNS of low Re flow over a pitching and plunging airfoil, varying the mean pitching angle (θ_m) and the phase shift between the pitching and plunging motions (ϕ). We have identified an optimal lift-and-thrust producing case ($\theta_m = 10°$, $\phi = 90°$), with a propulsive efficiency comparable to the thrust producing case used as a reference. In addition we have studied the effect of variations in ϕ and θ_m with respect to this optimal lift-and-thrust producing case. The effect of θ_m is more pronounced, increasing the lift as θ_m increases from 0° to 20°. However, there is a clear degradation in the thrust performance for $\theta_m > 10°$, associated with drag production during the upstroke.

References

[1] W. Shyy, Y. Lian, J. Tang, D. Viieru, and H. Liu, *Low Reynolds number flyers*. Cambridge University Press, 2008.
[2] S. P. Sane, "The aerodynamics of insect flight," *Journal of Experimental Biology*, vol. 206, no. 23, pp. 4191–4208, 2003.
[3] M. F. Platzer, K. D. Jones, J. Young, and J. S. Lai, "Flapping wing aerodynamics: progress and challenges," *AIAA journal*, vol. 46, no. 9, pp. 2136–2149, 2008.
[4] W. Shyy, H. Aono, S. K. Chimakurthi, P. Trizila, C.-K. Kang, C. E. Cesnik, and H. Liu, "Recent progress in flapping wing aerodynamics and aeroelasticity," *Progress in Aerospace Sciences*, vol. 46, no. 7, pp. 284–327, 2010.
[5] M. Uhlmann, "An immersed boundary method with direct forcing for the simulation of particulate flows," *J. Comput. Phys.*, vol. 209, no. 2, pp. 448 – 476, 2005.
[6] M. Moriche, "Development and validation of a numerical solver for unsteady aerodynamics applications," Master's thesis, Univ. Carlos III de Madrid, 2013.
[7] J. M. Anderson, "Vorticity control for efficient propulsion.," tech. rep., DTIC Document, 1996.